$$\left.\begin{aligned} v_j^+(\bar{x}_j,t_j) &= y'_{s+}(\bar{x}_j,t_j) \\ v_j^-(\bar{x}_j,t_j) &= y'_{s-}(\bar{x}_j,t_j) \end{aligned}\right\} \text{ on } S_j$$

$$v_j^+[(\bar{x}_j-\bar{x}_k),t_j] = v_j^-[(\bar{x}_j-\bar{x}_k),t_j] = 0 \quad \text{on } S_{j+k} \qquad k=1,N-1$$

$$v_j^+[(\bar{x}_j-\bar{x}_k),t_j] = v_j^-[(\bar{x}_j+\bar{x}_\ell),t_j] = 0 \quad \text{on } S_{j-\ell} \qquad \ell=1,N-1$$

$$\Delta C_{pj}(\bar{x}_j,t_j) = 0 \text{ on } w_j \tag{11}$$

where

$$C_p(\bar{x},t) = \sum_{-N}^{N} C_{pj}(\bar{x}_j,t) \tag{12}$$

and $y=y'_{s+}(\bar{x}_j,t_j)$ and $y=y'_{s-}(\bar{x}_j,t_j)$ denote the slopes on the upper and lower surfaces of the $j$th blade, respectively. It should be noted that in the $(\bar{x}_j,t_j)$ coordinate system each of elementary problems for $\phi_j$ is identical.

Periodicity is applied on the $j=\pm N$ blades and their wakes. The wake boundary condition is given by

$$\Delta C_{p_j}[(\bar{x}_j-\bar{x}_k),t_j] = 0 \text{ on } w_{j+k} \quad k=1,N-1$$

$$\Delta C_{p_j}[(\bar{x}_j+x_\ell),t_j] = 0 \text{ on } w_{j-\ell} \quad \ell=1,N-1 \tag{13}$$

This is equivalent to keeping all blades stationary except the $j$th blade and allows the relevant wave transmission through each blade wake. Note that the time is always $t_j$, the time associated with the $j$th blade. No interblade phase lag is required at this stage.

When $\phi_j$ are summed, together with the boundary conditions, the problem defined by Eqs. (5) and (10-13) is identical to the problem defined by Eqs. (1-4). Hence the problem for any time lag $t_0$ between blades can be constructed from the superposition of the elementary problem defined by Eqs. (9) and (11-13). The superposition mechanism is as follows.

Let the solution to the elementary problem for $j=0$ be given by $\phi_0(\bar{x},t)$. The solution for $\phi_j(\bar{x},t_j)$ is then given by

$$\phi_j(\bar{x}_j,t_j) = \phi_0(\bar{x},t) \tag{14}$$

Since the functional form of $\phi_0$ with both $\bar{x}$ and $t$ is known from the elementary solution for $j=0$, this reparameterization is trivial. The final solution for the zeroth blade is then given by Eqs. (5) and (14); thus

$$\phi(\bar{x},t) = \sum_{-N}^{N} \phi_0(\bar{x}-\bar{x}_j,\ t-jt_0) \tag{15}$$

Thus the complete time-dependent cascade flow for any interblade phase angle can be constructed by superposition of the elementary problem defined by Eqs. (5) and (10-13).

If $\phi(\bar{x},t)$ and its derivatives are continuous, a similar relation to Eq. (15) can be constructed for the pressure coefficient $C_p(\bar{x},t)$. In addition, similar formulas can be derived for the lift and moment coefficients.

The idea discussed above can be extended to discontinuous transonic flows using the method of strained coordinates.[1] Results are given by Kerlick and Nixon.[3]

## Conclusion

The main contribution to the computation time for an unsteady calculation of cascade flutter in a transonic flow is the need to repeat the calculation for a range of interblade phase angles. The present analysis shows how this problem can be eliminated by a judicious choice of elementary solutions.

## Acknowledgment

This work was sponsored by Naval Air Systems Command under Contract N00019-81-C-0169.

## References

[1] Nixon, D., "Notes on the Transonic Indicial Method," *AIAA Journal*, Vol. 16, June 1978, pp. 613-616.

[2] Verdon, J. M. and Caspar, J. R., "Subsonic Flow Past an Oscillating Cascade with Finite Mean Flow Deflection," *AIAA Journal*, Vol. 18, May 1980, pp. 540-548.

[3] Kerlick, G. D. and Nixon, D., "A High Frequency Transonic Small Disturbance Code for Unsteady Flows in a Cascade," AIAA Paper 82-0955, 1982.

# Finite Element Modeling Techniques for Constrained Layer Damping

R. E. Holman* and J. M. Tanner†
*Hughes Aircraft Company, El Segundo, California*

## Introduction

CONSTRAINED layer damping treatments are used to suppress noise and vibration in complex structural systems. These treatments provide effective suppression by dissipating energy in a soft, heavily damped, viscoelastic core sandwiched between the two face sheets of a composite panel in flexure.

A number of authors have considered analytical techniques to predict the performance of constrained layer damped beams and plates. Ross et al.[1] developed a fourth-order theory for simply supported composite beams which have a complex modulus core. Rao[2] formulated a sixth-order theory using an energy approach, and obtained exact solutions for these composite beams which have various boundary conditions.

Johnson et al.[3] developed a three-dimensional finite element plate model using the MSC/NASTRAN computer program. The base beam and the constraining layer were modeled by plate elements. The viscoelastic core was represented by solid elements. The material properties of the viscoelastic core were represented by a complex, frequency dependent, shear modulus $G(\omega)[1+i\eta(\omega)]$. They showed that the modal strain energy method could be used to accurately and efficiently solve this problem.

The modal strain energy method uses the undamped modal characteristics. Modal loss factors are computed using the relation

$$\eta_r = \left(\sum_e \eta_e \phi_{re}^T k_e \phi_{re}\right) \Big/ \left(\sum_e \phi_{re}^T k_e \phi_{re}\right) \tag{1}$$

where $\eta_r$ is the modal loss factor for the $r$th mode, $\phi_{re}$ the undamped modal vector for the $e$th element in the $r$th mode, $\eta_e$ the loss factor for the $e$th element, and $k_e$ the stiffness matrix for the $e$th element. This method offers the following advantages for the analysis of constrained layer damped structures.

1) The method's computational costs are reasonable because undamped modal characteristics are used.

Presented as Paper 81-0485 at the AIAA/ASME/ASCE/AHS 22nd Structures, Structural Dynamics and Materials Conference, Atlanta, Ga., April 9-10, 1981; submitted April 15, 1981; revision received July 26, 1982. 

*Senior Scientist.
†Massachusetts Institute of Technology Intern.

2) The method easily can be implemented on many commercial finite element codes.

3) The method provides the information required for the proper design of a damping treatment.

In this Note, new finite elements for constrained layer damped beams and rectangular plates will be developed using a displacement formulation based on a refined small deflection theory that allows core shear deformation. These 16 degree-of-freedom beam elements and 28 degree-of-freedom plate elements are smaller in size and require less machine time to generate than the 40 degree-of-freedom Johnson-Kienholz-Rodgers element. These new elements can be used in existing general purpose finite element computer codes that possess the capability to input a general stiffness matrix and to use the modal strain energy method. Numerical examples will be presented and compared with existing analytical results.

## Finite Element Formulation

A typical constrained-layer damped beam or plate consists of a base layer (1) and a constraining layer (3) which sandwich a soft, heavily-damped viscoelastic core (2), as shown in Fig. 1. The extensional and flexural rigidities are described by $B_1=E_1A_1$ and $D_1=E_1I_1$ for the base layer and by $B_3=E_3A_3$ and $D_3=E_3I_3$ for the constraining layer. The shear rigidity of the core is represented by $K_2=G_2A_2$.

The following assumptions are made in the derivation.

1) Displacements are small and continuous.

2) The face plates individually deform per Kirchhoff hypothesis.

3) The core is rigid in the direction normal to the face plates.

4) The core is flexible in the directions parallel to the face plates, deforms mainly in shear, and does not carry much axial force.

The strain energies for the beam element due to extension and flexure of the base and constraining layers, and due to shear of the core, can be written as[4]

$$U_1+U_3=\frac{1}{2}\int_0^L (Dw_{xx}^2+Bu_x^2)\,dx$$

$$U_2=\frac{1}{2}\int_0^L K_2(\alpha^2 w_x^2+2\alpha\beta w_x u+\beta^2u^2)\,dx \tag{2}$$

where $w$ is the normal displacement and $u$ the axial extension of the base layer and

$$B=B_1[1+(B_1/B_3)] \qquad D=D_1+D_3 \qquad \alpha=c/t_2$$

$$\beta=(1/t_2)[1+(B_1/B_3)] \qquad c=\tfrac{1}{2}(t_1+2t_2+t_3) \tag{3}$$

The face plate normal and in-plane displacement functions $w(x)$ and $u(x)$ for the 6 degree-of-freedom planar beam bending element are

$$w(x)=a_1+a_2x+a_3x^2+a_4x^3, \quad u(x)=a_5+a_6x \tag{4}$$

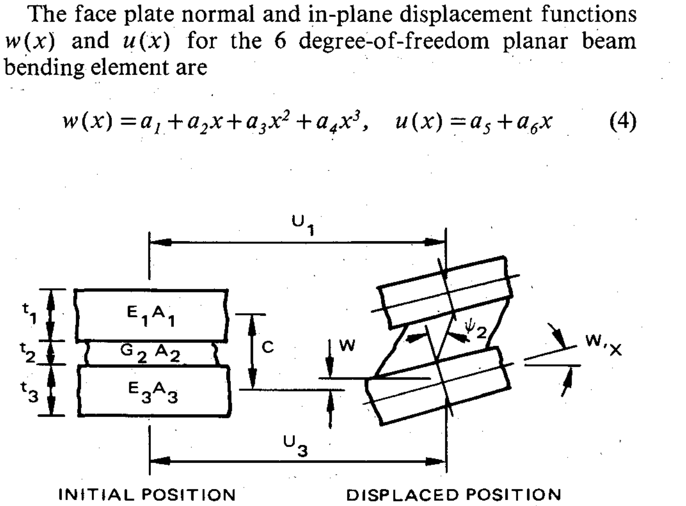


**Fig. 1 Sandwich beam geometry.**

These displacement functions can be expressed explicitly in terms of the nodal coordinates $\delta_i$ defined in Fig. 2. The stiffness matrices for the face sheets $[K]_f$ and the core $[K]_c$ can then be evaluated using the relations

$$[K]_f=\left[\frac{\partial^2}{\partial\delta_r\partial\delta_s}(U_1+U_3)\right] \qquad [K]_c=\left[\frac{\partial^2}{\partial\delta_r\partial\delta_s}(U_2)\right] \tag{5}$$

The strain energies for the plate element which result from the extension and flexure of the base and constraining layers as well as from the shear of the core can be written as follows.

$$U_1+U_3=\frac{1}{2}\int_0^b\int_0^a B\Big[u_x^2+v_y^2+2\nu u_xv_y + \left(\frac{1-\nu}{2}\right)(u_y+v_x)^2\Big]dxdy+\frac{1}{2}\int_0^b\int_0^a\frac{D}{1-\nu^2}[w_{xx}^2+w_{yy}^2 +2\nu w_{xx}w_{yy}+2(1-\nu)w_{xy}^2]\,dxdy$$

$$U_2=\frac{1}{2}\int_0^b\int_0^a K_2[\alpha^2(w_x^2+w_y^2)+2\alpha\beta(w_xu+w_yv) +\beta^2(u^2+v^2)]\,dxdy \tag{6}$$

where $w$ is the normal displacement and $u$ and $v$ the in-plane displacements of the base layer.

The face plate normal displacement function $w(x,y)$ and the in-plane displacement functions $u(x,y)$ and $v(x,y)$ for the 20 degree-of-freedom plate bending element are

$$w(x,y)=a_1+a_2x+a_3y+a_4x^2+a_5xy+a_6y^2+a_7x^3+a_8x^2y +a_9xy^2+a_{10}y^3+a_{11}x^3y+a_{12}xy^3$$

$$u(x,y)=a_{13}+a_{14}x+a_{15}y+a_{16}xy$$

$$v(x,y)=a_{17}+a_{18}x+a_{19}y+a_{20}xy \tag{7}$$

These displacement functions can be expressed explicitly in terms of the nodal coordinates $\delta_i$ of the rectangular plate defined in Fig. 3. The stiffness matrices for the face sheets $[K]_f$ and the core $[K]_c$ can then be evaluated using Eq. (5).

## Implementation in Computer Codes

These beam and plate finite elements can be used in existing general purpose finite element computer codes that possess

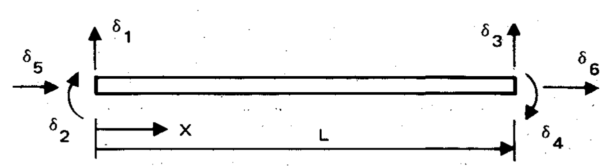


**Fig. 2 Beam coordinates.**

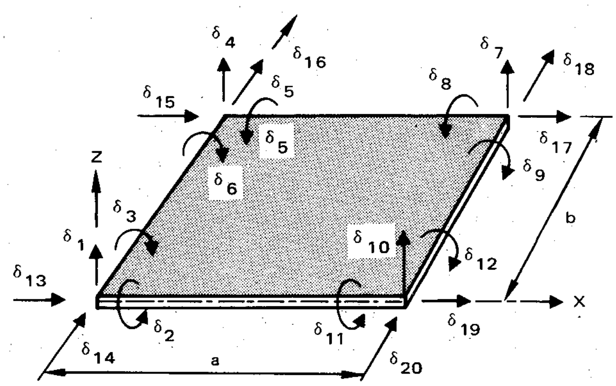


**Fig. 3 Plate coordinates.**

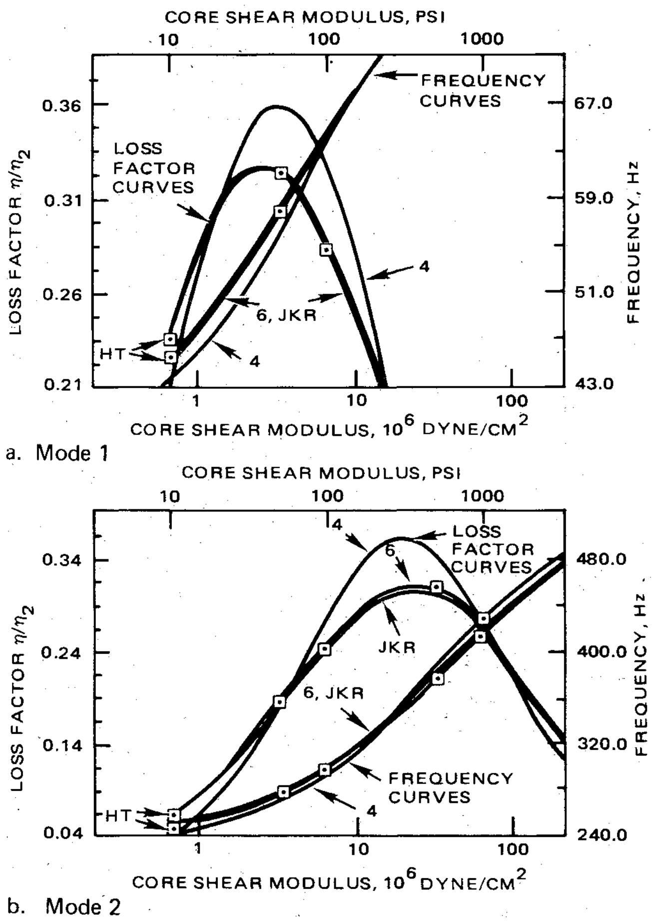


**Fig. 4 Loss factors and natural frequencies for cantilever beam using the fourth- and sixth-order theories and the Johnson-Kienholz-Rodgers and Holman-Tanner finite elements.**

the capability both to input a general stiffness matrix and to use the modal strain energy method. MSC/NASTRAN[5] has been used in this investigation. The model is generated in the conventional manner. More nodes provide the additional degrees-of-freedom required by these elements. These nodes coincide with the conventional element nodes, and their unused degrees-of-freedom are restrained. The required MSC/NASTRAN bulk data cards for these elements are created using a preprocessor. The input for this preprocessor is 1) connectivity cards identical to the CBAR and CQUAD4 cards, 2) property cards similar to the PBAR and PQUAD cards, and 3) GRID cards for the conventional element nodes. The output of this preprocessor is 1) the GENEL cards for the face sheet and core stiffness matrices, 2) the CONM2 cards for the lumped mass matrices, 3) the GRID cards for the locations of the additional nodes, and 4) the SPC cards for the restraints on the additional nodes.

The modal strain energy method can be used to efficiently solve this problem.[3] First, a standard modal extraction is executed and, then, the elastic strain energy in each element for each mode is calculated. Unfortunately, MSC/NASTRAN computes the strain energy in all elements except the GENEL element; nevertheless, MSC/NASTRAN's direct matrix abstraction programming (DMAP) capability can be used to compute the GENEL strain energies. The modal loss factors are then computed using Eq. (1). Finally, the modal loss factors are input via a damping vs frequency table for subsequent forced response calculations.

## Results

To evaluate the accuracy of the finite element representation, a series of calculations was performed using both the finite element model and the analytical theory. A 178-mm (7.00-in.) long by 12.7-mm (0.50-in.) wide cantilever beam with 1.27-mm (0.050-in.) thick aluminum face sheets and a 0.127-mm (0.005-in.) thick core was used in the analysis. The dimensions of this beam were those of the standard test specimen used to obtain material properties of viscoelastics by controlled vibration. The core's loss factor was held constant at 0.01 and its shear modulus was varied through a wide range of values.

The results are presented in Fig. 4 for the first two cantilever modes obtained from the fourth-order theory of Ross et al.,[1] the sixth-order theory of Rao,[2] and twenty element NASTRAN models, using the Johnson-Kienholz-Rodgers[3] and the Holman-Tanner[4] finite elements. The results are given for the modal loss factor $\eta$, normalized with respect to the core loss factor $\eta_2$, and the natural frequency. The sixth-order theory and the NASTRAN results are in excellent agreement, while those for the fourth-order theory differ somewhat, as was expected in view of the assumptions used in its derivation.

## References

[1]Ross, D., Ungar, E. E., and Kerwin, E. M. Jr., "Damping of Flexural Vibrations by Means of Viscoelastic Laminae," *Structural Damping*, Sec. III, ASME, New York, 1959.

[2]Rao, D. K., "Frequency and Loss Factors of Sandwich Beams Under Various Boundary Conditions," *Journal of Mechanical Engineering Science*, Vol. 20, May 1978, pp. 271-282.

[3]Johnson, C. D., Kienholz, D. A., and Rodgers, L. C., "Finite Element Prediction of Damping in Structures with Constrained Viscoelastic Layers," *Proceedings of the 51st Symposium on Shock and Vibration*, San Diego, Calif., Oct. 1980.

[4]Holman, R. E. and Tanner, J. M., "Finite Element Modeling Techniques for Constrained Layer Damping," AIAA Paper 81-0485, April 1981.

[5]McCormick, C. W., *MSC/NASTRAN User's Manual Version 60*, The MacNeal-Schwendler Corp., Los Angeles, Calif., 1980.

# Buckling of Very Thin, Nearly Perfect Axially Loaded Circular Cylindrical Shells

C. G. Foster*
*University of Tasmania, Hobart, Tasmania, Australia*

## Introduction

THE complex problem of predicting buckling loads for axially compressed cylindrical shells has defied any completely adequate explanation. Traditionally, the discrepancy between the classical load and the vast amount of experimental data available (e.g., as summarized by Hart-Smith[1]) has been attributed to end conditions and defects. The defects may be due to geometrical, metallurgical, or loading inconsistencies. However, very thin, expertly made shells (e.g., those of Babcock and Sechler[2]) collapse at loads substantially less than those predicted when end constraints are taken into account. A plausible explanation for this discrepancy is offered in terms of the space frame analogy for axial compression buckling previously developed by the author.[3-5]

Received Aug. 26, 1981; revision received June 24, 1982. 

*Senior Lecturer in Mechanical Engineering.